J. Biochem. **142,** 715–720 (2007)
doi:10.1093/jb/mvm184

Molecular Interaction of Ferredoxin and Ferredoxin-NADP$^+$ Reductase from Human Malaria Parasite

Yoko Kimata-Ariga[1,*], Takashi Saitoh[1,†], Takahisa Ikegami[1], Toshihiro Horii[2] and Toshiharu Hase[1]

[1]Institute for Protein Research, Osaka University, 3-2 Yamadaoka; and [2]Department of Molecular Protozoology, Research Institute for Microbial Diseases, Osaka University, Suita, Osaka 565-0871, Japan

Received July 2, 2007; accepted September 15, 2007; published online October 15, 2007

The malaria parasite possesses plant-type ferredoxin (Fd) and ferredoxin-NADP$^+$ reductase (FNR) in a plastid-derived organelle called the apicoplast. This Fd/FNR redox system, which potentially provides reducing power for essential biosynthetic pathways in the apicoplast, has been proposed as a target for the development of specific new anti-malarial agents. We studied the molecular interaction of Fd and FNR of human malaria parasite (*Plasmodium falciparum*), which were produced as recombinant proteins in *Escherichia coli*. NMR chemical shift perturbation analysis mapped the location of the possible FNR interaction sites on the surface of *P. falciparum* Fd. Site-specific mutation of acidic Fd residues in these regions and the resulting analyses of electron transfer activity and affinity chromatography of those mutants revealed that two acidic regions (a region including Asp26, Glu29 and Glu34, and the other including Asp65 and Glu66) dominantly contribute to the electrostatic interaction with *P. falciparum* FNR. The combination of Asp26/Glu29/Glu34 conferred a larger contribution than that of Asp65/Glu66, and among Asp26, Glu29 and Glu34, Glu29 was shown to be the most important residue for the interaction with *P. falciparum* FNR. These findings provide the basis for understanding molecular recognition between Fd and FNR of the malaria parasite.

Key words: ferredoxin, ferredoxin-NADP$^+$ reductase, human malaria parasite, NMR.

Abbreviations: cyt c, cytochrome c; Fd, ferredoxin; FNR, ferredoxin-NADP$^+$ reductase; HSQC, heteronuclear single-quantum correlation; PfFd, *P. falciparum* Fd; PfFNR, *P. falciparum* FNR.

Protozoan parasites of the phylum Apicomplexa, including *Plasmodium sp*. (the causative agent of malaria) and *Toxoplasma* sp., contain a non-photosynthetic plastid organelle called the apicoplast (*1*), which was acquired by secondary endosymbiosis of algae (*2*). The apicoplast was shown to be essential for the parasite's survival (*3*, *4*). The vital function of the apicoplast remains unclear, but it is thought to employ biosynthesis of fatty acids, isoprenoids, Fe-S clusters and haems, based on the analyses of the genome sequence (*5*).

We previously reported the cloning and characterization of plant-type ferredoxin (Fd) and Fd-NADP$^+$ reductase (FNR) from *Plasmodium falciparum* (human malaria parasite), which have been proposed as a redox system to supply reducing power in the apicoplast (*6*). FNR, an FAD-containing enzyme, is responsible for the reduction of Fd, a small 2Fe-2S protein, using reducing equivalents from NADPH. Fd in photosynthetic plastids (chloroplasts) receives electrons from photosystem I, and a large portion of this reduced Fd is utilized by FNR for the conversion of NADP$^+$ to NADPH, needed in the Calvin cycle (*7*). In non-photosynthetic plastids, on the other hand, FNR catalyses the reverse direction of electron transfer from NADPH to Fd, which then acts as a major reductant for various reactions in this organelle such as reduction of nitrite (*8*) and sulfite, and biosynthesis of unsaturated fatty acids. Photosynthetic and non-photosynthetic plant tissues contain distinct isoforms of both Fd and FNR, and the electron transfer cascade of NADPH–FNR–Fd in the direction opposite to that occurring in the photosynthetic process is facilitated by a combination of non-photosynthetic isoproteins of Fd and FNR (*9*, *10*). By analogy, a redox cascade of NADPH–FNR–Fd in the apicoplasts has been proposed to provide reducing power, which drives putative, possibly crucial, Fd-dependent metabolisms (*11*). The involvement of apicoplast Fd is indicated by the recent discovery of an Fe-S cluster assembly pathway (*12*), fatty acid desaturase (*11*) and isoprenoid biosynthesis pathway (*13*). Because this plant-type redox system is not present in the mammalian host, it would represent a promising drug target to combat malaria, for instance, by developing substances that inhibit the interaction between Fd and FNR.

Fd and FNR form a 1:1 complex, and X-ray crystal structures of the plant Fd-FNR complexes have been reported (*14*, *15*), clarifying the sites involved in complex formation between the Fd and FNR molecules. The basic pattern consists of a core of hydrophobic interactions surrounding the prosthetic groups, stabilized by a series

*To whom correspondence should be addressed. Tel: +81-6-6879-8611, Fax: +81-6-6879-8613,
E-mail: a-yoko@protein.osaka-u.ac.jp
†Present address: Digital Medicine Initiative, Kyushu University, Higashi-ku, Fukuoka 812-8582, Japan.

of interactions between charged side chains (negative charges of Fd and the positive charges of FNR) and through hydrogen bonds. However, the specific interaction mode of Fd and FNR, such as the orientation of Fd relative to FNR, is largely different between the Fd–FNR pairs of photosynthetic (leaf) type and non-photosynthetic (root) type (*15*). These distinct Fd–FNR interaction modes of leaf-type and root-type complexes may be due to optimization for their efficiency in photosynthetic and non-photosynthetic (heterotrophic) electron cascades, which are opposite in terms of the direction of electron flow (*15*).

The amino acid sequence of *P. falciparum* Fd (PfFd) shares about 50% homology with plant Fds (*11*, *16*), and its backbone structure, as solved by X-ray crystallography, closely resembles those of plant Fds (*6*). On the other hand, *P. falciparum* FNR (PfFNR) shares lower homology (20–30%) with plant FNRs, displaying unique large insertions and deletions (*17*), which appear to be responsible for the unique disordered surface structures shown by its recently solved crystal structure (*18*). PfFNR transfers electron to PfFd much more efficiently than it does to plant Fds (*6*), suggesting the advantageous combination. So far, 3D structure of PfFd–PfFNR complex is not available. In order to obtain detailed information about the molecular interaction between Fd and FNR in *P. falciparum*, we investigated the FNR-interaction site on PfFd using NMR structural analyses combined with site-directed mutagenesis of the Fd. For comparison, the interaction modes of PfFd with heterologous, plant FNRs were also investigated.

EXPERIMENTAL PROCEDURES

Preparation of Recombinant Proteins—Cloning and preparation of PfFd and PfFNR were described previously (*6*). The ^{15}N-labelled PfFd was obtained by culturing the bacterial cells in an M9 minimum medium containing $^{15}NH_4Cl$ as the sole nitrogen source. The ^{15}N- and ^{13}C-labelled PfFd was obtained by the same procedure, except that medium contained [$^{13}C_6$]-D-glucose and $^{15}NH_4Cl$.

NMR Spectroscopy—Recombinant PfFd was labelled uniformly with ^{15}N-, or ^{15}N- and ^{13}C-stable isotopes. The NMR spectra were recorded at 298K on a Bruker DRX 500 spectrometer operating at 500.13 MHz for the proton base frequency. The NMR samples used for the resonance assignments contained 2.0 mM ^{15}N- and ^{13}C-labelled PfFd in 90% H_2O and 10% D_2O containing 30 mM potassium phosphate (pH 7.0) and 100 mM KCl. The ^{1}H, ^{13}C and ^{15}N resonances were sequentially assigned using 2D double-resonance and 3D triple-resonance experiments through bond correlations: 2D ^{1}H-^{15}N heteronuclear single quantum correlation (HSQC), and 3D HNCACB and CBCA(CO)NH spectra. A series of 2D ^{1}H-^{15}N HSQC spectra of ^{15}N-labelled PfFd were recorded as a function of FNR concentration. The PfFd-containing solution (0.2 mM) was titrated with FNR at the molar ratios ([FNR]/[Fd]) of 0.25, 0.5 and 1.0 in a 25 mM potassium phosphate buffer (pH 7.0) containing 10 mM KCl. The resonances of free and bound forms of PfFd showed that the exchange between these forms was in a fast exchange mode on the NMR time scale for all the FNR/Fd stoichiometry. Weighted averages of the ^{1}H and ^{15}N chemical shift changes, $\Delta\delta^1H_N$ and $\Delta\delta^{15}N$, respectively, were calculated with the function of the form, $\Delta\delta = [(\Delta\delta_{1HN})^2 + (0.17 \times \Delta\delta_{15N})^2]^{1/2}$. All the spectra were processed with NMRPipe software (*19*) and analysed with Sparky software developed by T. D. Goddard and D. G. Kneller in University of California, San Francisco.

Site-directed Mutagenesis of PfFd—For construction of PfFd mutants, the QuikChange XL site-directed mutagenesis kit (Stratagene) was used according to the manufacturer's instructions. The synthetic oligonucleotides used for the mutagenesis were GAATATATTCTGAATGCTAGTCAACGTCAGAATGTTCAACTGC and GCAGTTGAACATTCTGACGTTGACTAGCATTCAGAATATATTC for D26N/E29Q/E34Q, GATCAGAGTTATCTGAATCAAGAGCAGATCAAG and CTTGATCTGCTCTTGATTCAGATAACTCTGATC for D65N/E66Q, GAAACGCACAAGCAAAACGAGCTCCACAACATGTAAGCTCTAG and CTAGAGCTTACATGTTGTGGAGCTCGTTTTGCTTGTGCGTTTC for E92Q/D93N/D97N, GGATGAAGAGCAGATCGCGGACGGATATATTCTGCTGTGTACC and GGTACACAGCAGAATATATCCGTCCGCGATCTGCTCTTCATCC for K70A/K71D/K72G, GGATGAAGAGCAGATCGAGGAAGGATATATTCTGCTGTGTACC and GGTACACAGCAGAATATATCCTTCCTCGATCTGCTCTTCATCC for K70E/K71E/K72G, GAATATATTCTGAATGCTAGTGAACGTC and GACGTTCACTAGCATTCAGAATATATTC for D26N, CTGGATGCTAGTCAACGTCAGAATGTTG and CAACATTCTGACGTTGACTAGCATCCAG for E29Q, and CGTCAGAATGTTCAACTGCCGTATAGTTG and CAACTATACGGCAGTTGAACATTCTGACG for E34Q, where the underlined bases denote changes from the wild-type sequence. The mutation sites and the sequence integrity of the entire coding region of PfFd were confirmed by DNA sequencing. All mutant Fds isolated from *Escherichia coli* cells were assembled with the 2Fe-2S cluster and showed absorption spectra comparable to that of wild-type PfFd.

Enzymatic Analysis—NADPH-dependent Fd reduction by FNR was measured as described by Onda *et al.* (*9*) except that the concentration of cytochrome *c* (cyt *c*) was lowered to 45 μM and light-path was increased to 1 cm when PfFNR was used.

Affinity Chromatography—Immobilized PfFNR was obtained by coupling 130 nmol of PfFNR to 600 mg of CNBr-activated-Sepharose 4B (GE Healthcare Bio-Science), following the manufacturer's directions. PfFNR-conjugated resin (2 ml) was packed and used as an affinity column in an FPLC apparatus. After equilibrating the column with 50 mM Tris–HCl, pH 7.5, wild-type and mutant PfFds (1–2 nmol) were loaded, and a linear gradient of NaCl was applied to elute the proteins at a flow rate of 0.5 ml/min. Elution of the proteins was monitored by absorption at 280 nm, and the conductivity of the eluate was correspondingly monitored.

RESULTS

Chemical Shift Perturbation of PfFd with PfFNR—The sites of PfFd that potentially interact with PfFNR were

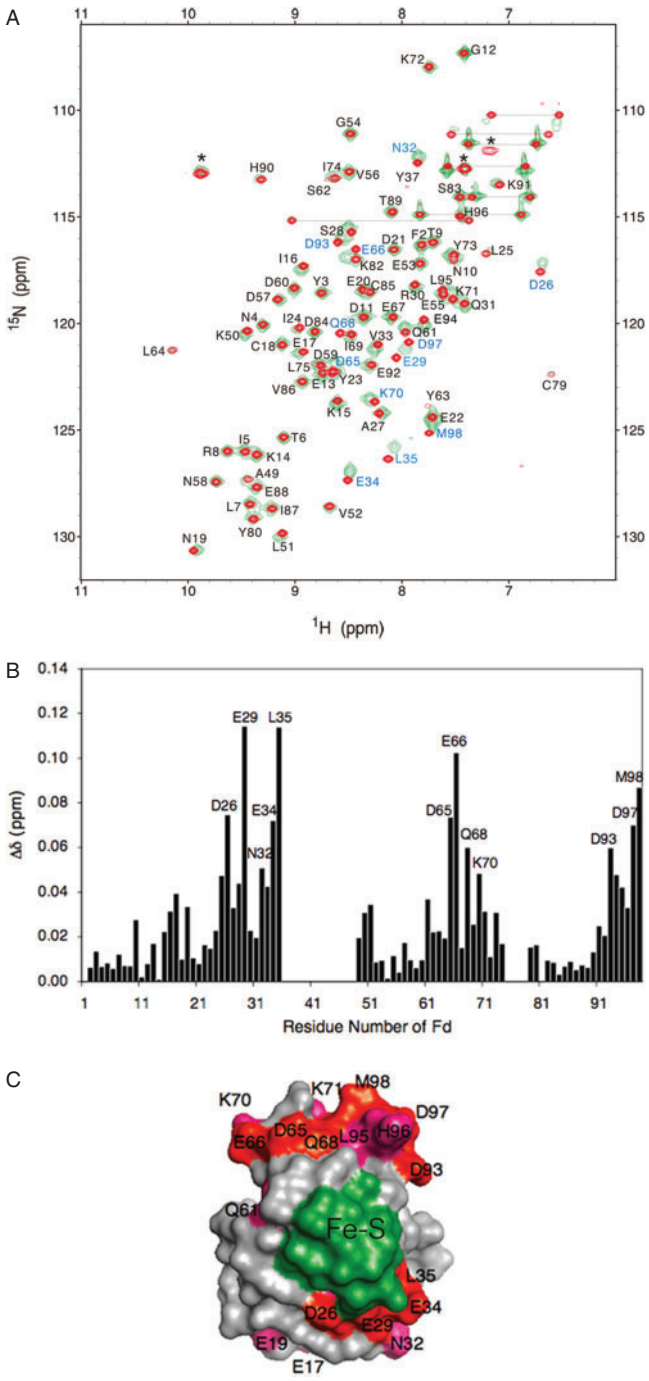

Fig. 1. **NMR chemical shift perturbation analysis of PfFd upon complex formation with PfFNR.** (A) Overlay of 2D ^{1}H-^{15}N HSQC spectra of ^{15}N-labelled PfFd in the absence (*red*) and the presence (*green*) of non-labelled PfFNR at a molar ratio ([FNR]/[Fd]) of 1.0. The assignments to the backbone amide groups are indicated in *black* for cross-peaks with no or little chemical shift change, and in *blue* for those with a significant change. The horizontal lines connect the peaks of the NH_2 moieties in the side chains of Gln and Asn residues. Asterisks indicate the aliasing peaks for ^{15}N dimension. (B) Weighted averages of the ^{1}H and ^{15}N chemical shift changes on the two HSQC spectra in panel A ($\Delta\delta$) plotted against the residue number. (C) Mapping of the chemical shift changes on the 3D structure of PfFd (Protein Data Bank entry 1IUE). Residues with chemical shift changes ($\Delta\delta$) > 0.06 p.p.m. and 0.03–0.06 p.p.m. are shown in *red* and *magenta*, respectively. Residues near the 2Fe-2S cluster, whose chemical shift data are not available due to the paramagnetic effect of the iron, are shown in *green*. This region mostly corresponds to the hydrophobic area around the 2Fe-2S cluster, which presumably consists of the core of interaction site with FNR. The figure was produced with PyMOL (*24*).

analysed in solution in an NMR chemical shift perturbation experiment (Fig. 1). A series of HSQC spectra of ^{15}N-labelled PfFd was measured as a function of the molar ratios of non-labelled PfFNR to PfFd. As shown in Fig. 1A, the amide resonance of most Fd residues (red spots) was well observed except for those in two regions: Ser38 to Ala48 and Leu76 to Thr78, whose signals were hardly detectable due to paramagnetic relaxation enhancement caused by the 2Fe-2S cluster of Fd. A general broadening of the resonance signals and concomitant chemical shift changes only for certain residues occurred upon addition of PfFNR (green spots in Fig. 1A). For each amide group of PfFd, the changes in the ^{1}H and ^{15}N chemical shifts were combined according to the equation described under "EXPERIMENTAL PROCEDURES section", and resulting values are shown in Fig. 1B. Large chemical shift changes were observed in three regions around Asp26-Leu35, Asp65-Gln68 and the C-terminus, all of which contained multiple acidic residues (Fig. 1B). Three-dimensional mapping of the Fd residues (Fig. 1C) that exhibited significant chemical shift perturbations (>0.06 p.p.m. shown in red and 0.03–0.06 p.p.m. shown in magenta) shows that these regions are distributed in areas surrounding the 2Fe-2S cluster, with the acidic residues mostly located on the surface of the Fd molecule.

Besides the above three regions, residues around Lys70 exhibited a relatively large chemical shift change (Fig. 1B). This region overlaps three successive lysine residues (Lys70, 71 and 72) that are unique to *Plasmodium* Fds (*6*).

Mutational Analysis of PfFd for Interaction with PfFNR—In order to verify whether the acidic residues in the three regions of PfFd that showed large NMR chemical shift changes contribute to the interaction with PfFNR, we prepared three PfFd mutants, D26N/E29Q/E34Q, D65N/E66Q and E92Q/D93N/D97N Fds, by substitution of multiple acidic residues in each region to the corresponding amide form. Then their electron transfer activity with PfFNR and physical binding ability to PfFNR were examined by kinetic analysis (Table 1) and affinity chromatography on PfFNR-immobilized Sepharose resin (Fig. 2A), respectively. Among the three mutants, D26N/E29Q/E34Q and D65N/E66Q Fds showed a significantly lower electron transfer efficiency compared to wild-type Fd as judged from kinetic parameters in Table 1. The D26N/E29Q/E34Q mutant showed the largest K_m value and, in agreement with this, it eluted from the PfFNR-immmobilized column much faster (even before the NaCl gradient was applied) than those of other mutant and wild-type PfFds (Fig. 2A), indicating that these acidic residues make a large contribution to the interaction with PfFNR. The D65N/E66Q mutant also showed reduced affinity for PfFNR-immobilized column, but to a lesser extent than the

Table 1. **Kinetic parameters for NADPH-dependent cytochrome *c* reduction catalysed by *P. falciparum* FNR, mediated by wild-type and mutant *P. falciparum* Fds.**

Fd form	K_m μM Fd	k_{cat} $e^- eq\, s^{-1}$
Wild-type	2.19 ± 0.36	20.6 ± 1.9
D26N/E29Q/E34Q	10.25 ± 1.61	21.2 ± 3.6
D65N/E66Q	7.24 ± 1.11	24.9 ± 0.6
E92Q/D93N/D97N	2.82 ± 0.43	33.7 ± 1.9
D26N	3.14 ± 0.32	27.4 ± 0.8
E29Q	5.39 ± 0.07	22.2 ± 0.3
E34Q	2.39 ± 0.18	21.4 ± 0.4
K70A/K71D/K72G	2.13 ± 0.63	16.6 ± 0.6
K70E/K71E/K72G	2.07 ± 0.51	18.6 ± 0.7

These data were extracted from the Fd saturation curves. The K_m and k_{cat} for Fds were determined from a double-reciprocal plot. The values are means ± SD of three independent determinations.

D26N/E29Q/E34Q mutant, which agrees with the result of kinetic analysis. The E92Q/D93N/D97N mutation showed slight increase in K_m and somewhat reduced affinity for PfFNR-immobilized column. The physical PfFNR-binding of E92Q/D93N/D97N mutant on the column appears to be relatively weaker than expected from the kinetic results. The reason for this phenomenon is not clear at present. Based on these results, we conclude that Asp26/Glu29/Glu34 and Asp65/Glu66 are important for the interaction with PfFNR and that the contribution of Glu92/Asp93/Asp97 for the interaction is small or insignificant judging from the kinetic results.

Large increase in k_{cat} was observed for E92Q/D93N/D97N mutant, which may reflect that this mutation could affect the process of electron transfer, for instance, by altering redox potential of the 2Fe-2S cluster. Significant (67–93 mV) increase in redox potential has been reported by substitution of acidic residues at the C-terminal region of maize root Fd [E93Q, (*20*)], spinach leaf Fd [E92A and E92K, (*21*)] and *Anabaena* Fd [E94K, (*22*)].

In order to further investigate which residue among Asp26, Glu29 and Glu34 mostly contributes to the FNR interaction, single-site mutants of D26N, E29Q and E34Q were prepared and analysed (Table 1 and Fig. 2B). Among the three single-site mutants, E29Q showed the largest change in K_m, D26N showed a less, but significant increase in K_m, and for E34Q, a marginal effect on K_m was seen (Table 1). In agreement with this, affinity chromatography on PfFNR-immobilized resin (Fig. 2B) showed that E29Q eluted the fastest, D26N was the next, and E34Q eluted slightly faster than wild-type. Thus, Glu29 was shown to be the most important residue for the interaction with PfFNR, and Asp26, and possibly Glu34, also was shown to have some contribution. In both analyses, single-site mutants conferred moderate effect compared to D26N/E29Q/E34Q mutant, indicating that the additive effect of the each three (or two) substitution conferred a larger effect as observed with D26N/E29Q/E34Q mutant.

We also prepared PfFd mutants of the three Lys repeats at 70–72, unique to *Plasmodium* Fds, where a moderate change of chemical shift was detected upon PfFNR binding (Fig. 1B). This repeat was changed to the

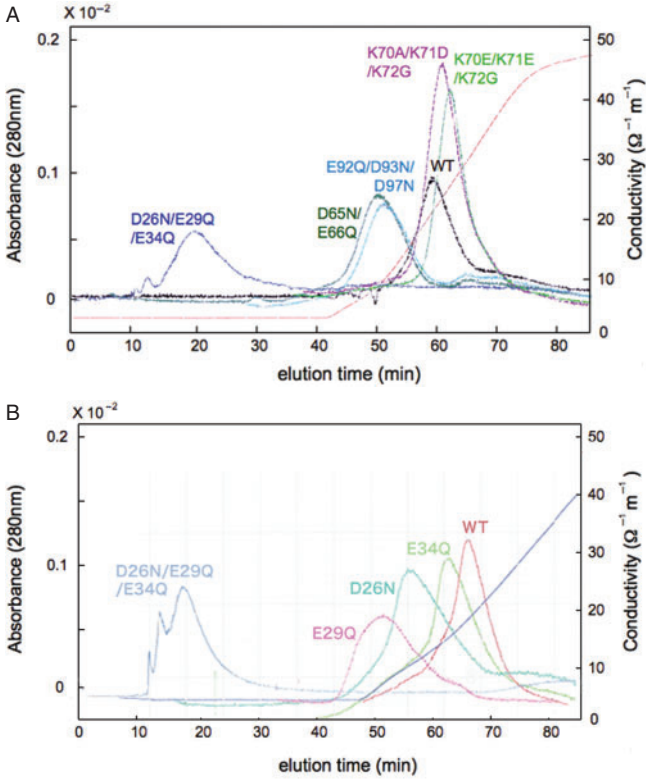

Fig. 2. **Affinity chromatography of wild-type and mutant PfFds on a PfFNR-immobilized column.** Conditions for the chromatography are described under "Experimental Procedures section". Elution profiles are shown for wild-type and PfFd mutants as a function of conductivity (red line for A, or blue line for B). Linear gradient of NaCl from 0 to 250 mM for the multiple-site mutants (A), or from 0 to 200 mM for the single-site mutants (B) was applied.

sequence of maize leaf Fd (Ala/Asp/Gly) and root Fd (Glu/Glu/Gly) at the corresponding site, and the resulting mutants showed a marginal change in interaction properties with FNR (Table 1 and Fig. 2A). Therefore, basic residues at positions 70–72 do not seem to contribute to FNR binding. These residues may be the interaction sites for other Fd-dependent redox proteins in the apicoplast of *Plasmodium* sp.

Chemical Shift Perturbation of PfFd with Plant FNRs—PfFd can receive electrons with a similar efficiency from both PfFNR and plant FNRs (*6*). In order to compare the interaction mode of PfFd with PfFNR and plant FNRs, NMR chemical shift perturbation experiments were performed using PfFd in combination with maize root FNR or maize leaf FNR as partner enzymes (Fig. 3A and B lower parts). The resulting chemical shift perturbation patterns varied from that obtained with PfFNR (Fig. 3A and B upper parts, same as Fig. 1B) in terms of the distribution of the shift changes; large changes in the C-terminus region were only observed with root FNR, while changes in the Asp65-Gln68 region were largest with leaf FNR. The chemical shift pattern with leaf FNR is similar to that of previous analysis with the leaf Fd/leaf FNR combination, where the region around Asp65 shows the largest change (*14*). NMR data

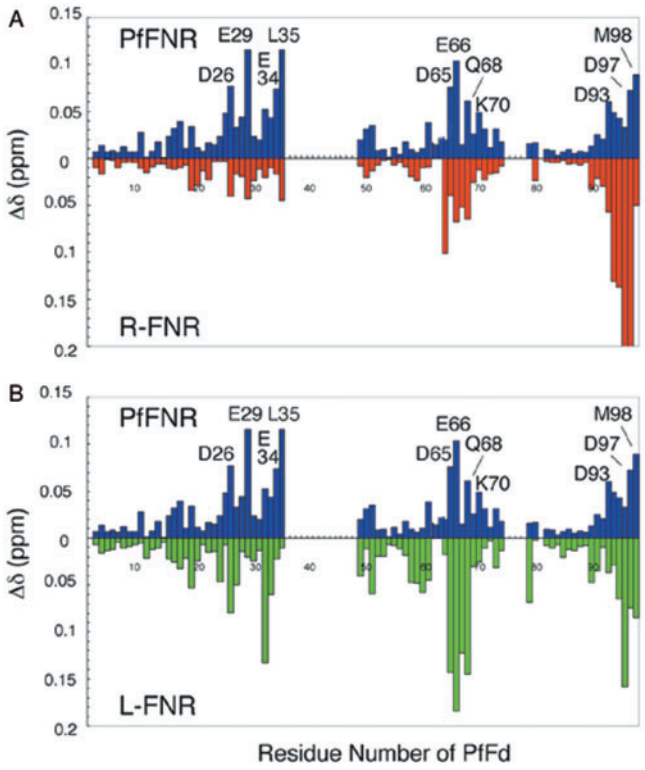

Fig. 3. **Comparison of NMR chemical shift changes.** The comparison of NMR chemical shift changes of PfFd upon complex formation with PfFNR (upper parts of A and B, same as Fig. 1B), maize root FNR (R-FNR) (lower part of A) and maize leaf FNR (L-FNR) (lower part of B).

for the root Fd/root FNR combination is not available yet. The large chemical shift perturbation of the C-terminal region of PfFd with root FNR may be due to a large movement of this region upon complex formation, because PfFd is longer than root Fd by two residues at the C-terminus, and root FNR may strongly interact with this extra part of PfFd. Thus, the three types of FNR appear to each have at least partly specific features in their interaction mode with PfFd.

It is noteworthy that, among the three combinations, the chemical shift pattern in the Asp26-Leu35 region is relatively more similar between PfFNR and root FNR (note the peaks at D26, E29 and L35 in Fig. 3A), suggesting similarity in local interaction mode.

DISCUSSION

In higher plant, photosynthetic and non-photosynthetic plant tissues contain distinct isoforms of both Fd and FNR, which are functionally differentiated (*9*, *10*, *15*). Crystal structures of both leaf- and root type Fd-FNR complexes have been solved, and the specific interaction mode of Fd and FNR, such as the orientation of Fd relative to FNR, was shown to be largely different between the two types of complexes (*14*, *15*). Because the clarified FNR-binding sites on Fd molecule, corresponding to acidic residues surrounding 2Fe-2S cluster, are mostly conserved between leaf and root types of Fd, the difference in their interaction mode appears to be mainly due to the differences in the Fd-binding residues on FNR molecules, which are specific to each type (*15*). Five ionic bridges stabilized the leaf complex, and among them two salt bridges of Fd-Glu65/FNR-Lys91 and Fd-Glu66/FNR-Lys88 were shown to dominantly contribute to the electrostatic interaction of Fd and FNR (*14*, *20*). In the root complex, on the other hand, three ionic bridges of Fd-Glu30/FNR-156, Fd-Glu35/FNR-310 and Fd-Asp67/FNR-Lys84 together with several hydrogen bonding pairs stabilize the relative orientation of the proteins (*15*).

With regard to *P. falciparum* proteins, backbone structure of PfFd closely resembles those of plant Fds, and the acidic residues surrounding the 2Fe-2S cluster are also highly homologous to plant Fds (*6*). On the other hand, PfFNR has unique structural properties (*18*), and residues that correspond to Fd-binding sites of either leaf- or root-type are not well conserved. In the current study, we investigated the PfFNR-binding sites on PfFd molecule using NMR chemical shift perturbation. Large chemical shift changes were observed in three regions (Asp26-Leu35, Asp65-Gln68 and the C-terminus), and the extent of changes was similar among the three, with slightly higher in the Asp26-Leu35 region (Fig. 1B). Following site-directed mutagenesis showed that the combination of the acidic residues of Asp26/Glu29/Glu34 conferred the large contribution to the interaction with PfFNR in both kinetic and physical binding analyses (Table 1 and Fig. 2), and that the degree of contribution among the three residues is in the order of Glu29>Asp26>Glu34. The acidic residues of Asp65/Glu66 are also important for the interaction with PfFNR, but to a lesser extent than Asp26/Glu29/Glu34. On the other hand, the contribution of Glu92/Asp93/Asp97 appears to be small. Because Asp65/Asp66 of leaf Fd are known to be the major interaction sites with leaf FNR (*14*, *23*), these combined data of NMR analyses and site-directed mutagenesis revealed the differences in the major FNR-interaction sites of Fd between plant (leaf type) and *P. falciparum*. There may exist salt bridges and/or hydrogen bonds between some of Asp26, Glu29 and Glu34 of PfFd residues and PfFNR residues, in analogy to the case of root Fd/root FNR complex, which is stabilized by three salt bridges involving Glu30, Glu35 Asp67 of Fd residues (corresponding to Glu29, Glu34 and Asp66 of PfFd) and several hydrogen bonds including Asp27 (corresponding to Asp26 of PfFd) (*15*). In this context, interaction mode of PfFd/PfFNR may be more similar to root complex than leaf complex, which appears to be reasonable if the interaction mode is related to the direction of physiological electron transfer. The local similarity of the chemical shift pattern in the Asp26-Leu35 region between the PfFd/PfFNR and PfFd/root FNR (Fig. 3A) also suggests their similarity of interaction mode in the region around Asp26, Glu29 and Glu34.

To conclude, in this study, acidic residues in two regions (Asp26/Glu29/Glu34 and Asp65/Glu66) surrounding the 2Fe-2S cluster of PfFd were shown to be important for the electrostatic interaction with PfFNR. The combination of Asp26/Glu29/Glu34 conferred larger contribution than that of Asp65/Glu66, and among Asp26, Glu29 and Glu34, Glu29 was shown to be the most important residue for the interaction with

P. falciparum FNR. Asp26, and possibly Glu34, also have some contribution. These findings provide the basis for understanding molecular recognition between Fd and FNR of the malaria parasite.

This work was supported by grant in aids for Creative Scientific Research (15GSO320) and for Scientific Research on Priority Areas (13225001) from the Ministry of Education, Culture, Sports, Science and Tsechnology of Japan.

REFERENCES

1. McFadden, G.I., Reith, M.E., Mulholland, J., and Lang-Unnasch, N. (1996) Plastid in human parasites. *Nature* **381**, 482
2. Köhler, S., Delwiche, C.F., Denny, P.W., Tilney, L.G., Webster, P., Wilson, R.J., Palmer, J.D., and Roos, D.S. (1997) A plastid of probable green algal origin in apicomplexan parasites. *Science* **275**, 1485–1489
3. Fichera, M.E. and Roos, D.S. (1997) A plastid organelle as a drug target in apicomplexan parasites. *Nature* **390**, 407–409
4. McFadden, G.I. and Roos, D.S. (1999) Apicomplexan plastids as drug targets. *Trends Microbiol.* **7**, 328–333
5. Ralph, S.A., van Dooren, G.G., Waller, R.F., Crawford, M.J., Fraunholz, M.J., Foth, B.J., Tonkin, C.J., Roos, D.S., and McFadden, G.I. (2004) Metabolic maps and functions of the *Plasmodium falciparum* apicoplast. *Nature Rev. Microbiol.* **2**, 203–216
6. Kimata-Ariga, Y., Kurisu, G., Kusunoki, M., Aoki, S., Sato, D., Kobayashi, T., Kita, K., Horii, T., and Hase, T. (2007) Cloning and characterization of ferredoxin and ferredoxin-NADP$^+$ reductase from human malaria parasite. *J. Biochem.* **141**, 421–428
7. Knaff, D.B. (1996) Ferredoxin and ferredoxin-dependent enzymes. in *Oxygenic Photosynthesis: The Light Reactions* (Ort, D.R. and Yocum, C.F., eds.) pp. 333–361 Kluwer Academic Publishers, Dordrecht.
8. Suzuki, A., Oaks, A., Jacquot, J.-P., Vidal, J., and Gapal, P. (1985) An electron transport system in maize roots for reaction of glutamate synthase and nitrite reductase: physiological and immunological properties of the electron carrier and pyridine nucleotide reductase. *Plant Physiol.* **78**, 374–378
9. Onda, Y., Matsumura, T., Kimata-Ariga, Y., Sakakibara, H., Sugiyama, T., and Hase, T. (2000) Differential interaction of maize root ferredoxin: NADP$^+$ oxidoreductase with photosynthetic and non-photosynthetic ferredoxin isoproteins. *Plant Physiol.* **123**, 1037–1045
10. Hanke, G.T., Kimata-Ariga, Y., Taniguchi, I., and Hase, T. (2004) A post genomic characterization of Arabidopsis ferredoxins. *Plant Physiol.* **134**, 255–264
11. Vollmer, M., Thomsen, N., Wiek, S., and Seeber, F. (2001) Apicomplexan parasites possess distinct nuclear-encoded, but apicoplast-localized, plant-type ferredoxin-NADP$^+$ reductase and ferredoxin. *J. Biol. Chem.* **276**, 5483–5490
12. Seeber, F. (2002) Biogenesis of iron-sulphur clusters in amitochondriate and apicomplexan protists. *Int. J. Parasitol.* **32**, 1207–1217
13. Rohrich, R.C., Englert, N., Troschke, K., Reichenberg, A., Hintz, M., Seeber, F., Balconi, E., Aliverti, A., Zanetti, G., Kohler, U., Pfeiffer, M., Beck, E., Jomaa, H., and Wiesner, J. (2005) Reconstitution of an apicoplast-localised electron transfer pathway involved in the isoprenoid biosynthesis of *Plasmodium falciparum*. *FEBS Letters* **579**, 6433–6438
14. Kurisu, G., Kusunoki, M., Katoh, E., Yamazaki, T., Teshima, K., Onda, Y., Kimata-Ariga, Y., and Hase, T. (2001) Structure of electron transfer complex between ferredoxin and ferredoxin-NADP$^+$ reductase. *Nat. Struct. Biol.* **8**, 117–121
15. Hanke, G.T., Kurisu, G., Kusunoki, M., and Hase, T. (2004) Fd:FNR electron transfer complexes: evolutionary refinement of structural interactions. *Photosynthesis Res.* **81**, 317–327
16. Pandini, V.H., Caprini, G., Thomsen, N., Aliverti, A., Seeber, F., and Zanetti, G. (2002) Ferredoxin-NADP$^+$ reductase and ferredoxin of the protozoan parasite *Toxoplasma gondii* interact productively *in vitro* and *in vivo*. *J. Biol. Chem.* **277**, 48463–48471
17. Bednarek, A., Wiek, S., Lingelbach, K., and Seeber, F. (2003) *Toxoplasma gondii*: analysis of the active site insertion of its ferredoxin-NADP$^+$ reductase by peptide-specific antibodies and homology-based modeling. *Exp. Parasitol.* **103**, 68–77
18. Milani, M., Balconi, E., Aliverti, A., Mastrangelo, E., Seeber, F., Bolognesi, M., and Zanetti, G. (2007) Ferredoxin-NADP$^+$ reductase from *Plasmodium falciparum* undergoes NADP$^+$-dependent dimerization and inactivation: functional and crystallographic analysis. *J. Mol. Biol.* **367**, 501–513
19. Delaglio, F., Grzesiek, S., Vuister, G.W., Zhu, G., Pfeifer, J., and Bax, A. (1995) NMRPipe: a multidimensional spectral processing system based on UNIX pipes. *J. Biomol. NMR* **6**, 277–293
20. Akashi, T., Matsumura, T., Ideguchi, T., Iwakiri, K., Kawakatsu, T., Taniguchi, I., and Hase, T. (1999) Comparison of the electrostatic binding sites on the surface of ferredoxin for two ferredoxin-dependent enzymes, ferredoxin-NADP+ reductase and sulfite reductase. *J. Biol. Chem.* **274**, 29399–29405
21. Aliverti, A., Faber, R., Finnerty, C.M., Ferioli, C., Pandini, V., Negri, A., Karplus, P.A., and Zanetti, G. (2001) Biochemical and crystallographic characterization of ferredoxin-NADP+ reductase from nonphotosynthetic tissues. *Biochemistry* **40**, 14501–14508
22. Hurley, J.K., Weber-Main, A.M., Stankovich, M.T., Benning, M.T., Thoden, J.B., Vanhooke, J.L., Holden, H.M., Kee Chae, Y., Xia, B., Cheng, H., Markeley, J.L., Martinez-Julves, M., Gomez-Moreno, C., Schmeits, J.L., and Tollin, G. (1997) Structure-function relationships in *Anabaena* ferredoxin: correlations between X-ray crystal structures, reduction potentials, and rate constants of electron transfer to ferredoxin:NADP$^+$ reductase for site-specific ferredoxin mutants. *Biochemistry* **36**, 11100–11117
23. Matsumura, T., Kimata-Ariga, Y., Sakakibara, H., Sugiyama, T., Murata, H., Takao, T., Shimonishi, Y., and Hase, T. (1999) Complementary DNA cloning and characterization of ferredoxin localized in bundle-sheath cells of maize leaves. *Plant Physiol.* **119**, 481–488
24. DeLano, W.L. (2002) The PyMOL Molecular Graphics System. DeLano Scientific, San Carlos, CA, USA. http://www.pymol.org.